Submitted to the Astrophysical Journal: April 22, 2002;
Revised June 25, 2002

Possible Identifications for Southern EGRET Sources

M. Tornikoski[1] and A. Lähteenmäki

Metsähovi Radio Observatory, Metsähovintie 114, FIN–02540 Kylmälä, Finland

M. Lainela

Väisälä Institute of Space Physics and Astronomy, Tuorla Observatory, FIN–21500 Piikkiö, Finland

E. Valtaoja

Väisälä Institute of Space Physics and Astronomy, Tuorla Observatory, FIN–21500 Piikkiö, Finland
and: Dept. of Physical Sciences, University of Turku, FIN–20100 Turku, Finland

ABSTRACT

We have made total flux density observations at high radio frequencies (90 and 230 GHz) of 12 Southern AGNs that were classified as possible ERGET identifications in the Third EGRET Catalog. Our observations confirm the blazar-nature of five of them. We have also studied sources that we considered good candidates for AGN counterparts of previously unidentified EGRET sources and which had not been observed in the millimeter-domain before. Four of them showed millimeter-range activity which may be related to their gamma-ray activity, making them good candidates for the EGRET source identification.

Subject headings: galaxies: active – gamma-rays: observations – quasars: general – radio continuum: galaxies

[1]Email: Merja.Tornikoski@Hut.Fi

1. Introduction

The third catalog of high-energy gamma-ray sources detected by EGRET (Hartman et al. 1999), hereafter 3EG, includes 271 sources. 66 of them are high-confidence identifications of blazar-type active galactic nuclei (AGNs): BL Lac objects, flat-spectrum radio qusars, or unidentified flat-spectrum radio sources, and 27 of them are lower-confidence potential blazar identifications. 170 sources (96 of which have $|b| > 10°$) in 3EG were not identified firmly with known objects.

The identification of the EGRET source counterparts is difficult because the source of the gamma-ray emission is not well located. The sources classified as possible AGN identifications in 3EG are questionable, either because the objects have low radio flux density (5 GHz data from the literature with $S < 300$ mJy) or because they lie outside the 95% uncertainty contour, sometimes even outside the 99% contour.

Because so many EGRET-detected sources have been identified with blazars, it is a natural hypothesis that some of the unidentified EGRET sources are also blazars. Several earlier papers have been published that present methods to try to identify unidentified EGRET sources with AGNs (e.g., Mattox et al. 1997; Punsly 1997; Bloom et al. 1997; Zook et al. 1997; Combi et al. 1999; Mattox et al. 2001).

We had two major goals in this project: we wanted to make further studies of probable/potential candidates already suggested in the literature, and we also wanted to propose possible new candidates for the unidentified sources listed in 3EG and to study a sample of those candidates to see if our method of using millimeter-wavelength observations is feasible for making new identifications.

In Section 2 we describe our observations. In Section 3 we discuss the method of identifying EGRET sources using millimeter-domain data. In Section 4 we present our results for 12 Southern sources classified as potential blazar identifications in 3EG, in Section 5 we present the results for some sources suggested for the EGRET source counterparts earlier in the literature, and in Section 6 we present the results for a set of sources we identified as possible counterparts for the previously unidentified EGRET sources. The conclusions are given in Section 7.

2. Millimeter observations

The aim of this project was to study the high radio-frequency data of the potential EGRET counterpart AGNs in order to see if they are bright and variable, with flat or even inverted high-frequency part of the radio spectrum, and thus good candidates for the EGRET identifications. For the sources with long data sets we also wanted to study if they were going through a flaring stage at high radio frequencies at the time of the EGRET-detection.

Our group has been studying AGNs at high radio-frequencies since 1987 with the 15-meter Swedish–ESO Submillimeter Telescope (SEST) at the European Southern Observatory (ESO) site of La Silla, Chile, latitude 29° South. The observing frequencies were 90 GHz (3 mm) and 230 GHz (1.3 mm). Originally, the observations were made as described in Tornikoski et al. (1996), but since June 1994 an SIS mixer receiver was used for the 90 GHz observations instead of the Schottky receiver. The bolometer was used for the majority of the 230 GHz observations, resulting in improved sensitivity compared to the Schottky/AOS setup used earlier.

During our various observing projects with the SEST we have observed both well-known strong and variable sources as well as some samples of rarely observed sources (e.g., Tornikoski et al. 1993, 1999, 2000b, 2001); details about the SEST AGN monitoring observations can be found in Tornikoski et al. (1996) and Tornikoski (2002, in preparation). For some of the objects studied in this paper (many of the sources studied in Section 4) we have millimeter-wave monitoring data spanning a decade, giving us a very good estimate of their variability behavior over a very long period of time. Most of the objects studied in Section 5 and Section 6 had never been observed in the millimeter-domain before, and for this paper we observed them at 90 GHz in April 2000 and August 2000.

For the plots and tables in this paper our SEST data sets were complemented with multifrequency radio data from the literature. These data are from Kuehr et al. (1981); Lawrence et al. (1983); Salonen et al. (1987); Teräsranta et al. (1987); Steppe et al. (1988); Wright & Otrupcek (1990); Large et al. (1991); Wright et al. (1991); Teräsranta et al. (1992); Steppe et al. (1992, 1993); Tornikoski et al. (1993); Bramwell (1993); Ghosh et al. (1994); Bondi et al. (1996); Beasley et al. (1997); Bloom et al. (1997); Drinkwater et al. (1997); Zook et al. (1997); Reuter et al. (1997); Reich et al. (1998); Teräsranta et al. (1998); Kovalev et al. (1999); Reich et al. (2000); Teräsranta et al. (2001).

3. Background

Practically all EGRET-detected AGNs identified so far are bright and variable in the millimeter range, but all radio-bright and variable AGNs have not been detected by EGRET. Our earlier work (Valtaoja & Teräsranta 1996; Lähteenmäki et al. 1997; Tornikoski et al. 1999; Lähteenmäki et al. 2000; Tornikoski et al. 2000a) has shown that there seems to be a connection between the high radio-frequency and EGRET gamma-ray activity, and that the most probable blazar to be detected with EGRET is a source with an ongoing and still rising high-frequency radio flare.

The case of PKS 2255−282 (Tornikoski et al. 1999) demonstrates that an AGN can remain undetected by EGRET until it goes through an activity period which is observed both in the radio domain and at the gamma-ray energies. Thus it is highly possible that several of the unidentified EGRET sources in 3EG will turn out to be radio loud AGNs which probably would have shown also millimeter-wavelength activity at the time of the EGRET detection.

To summarize the millimeter-properties of the known EGRET blazars, we have collected in Table 1 the 5 GHz, 22 GHz and 90 GHz data for all of the EGRET-detected sources in 3EG with a high-confidence identification with an AGN (marked as "A", an AGN, in 3EG). The table lists the flux density minima and maxima as well as the number of data points at each frequency band, respectively. For the sources with at least one good-quality (signal-to-noise-ratio > 4) data point at two of these frequencies, we have calculated the spectral index α (using $S \propto \nu^{\alpha}$). Many of these sources have been standard targets of our AGN monitoring projects with the SEST telescope at 90 GHz, and as shown in the table, for many of these sources we have as many as over a hundred data points. Because especially the 90 GHz fluxes of these sources can radically vary between the quiet and the active states, we have calculated two different spectral indices: the α_{quiet} is calculated using the minimum flux densities at both 5 and 90 GHz, illustrating the shape of the assumed quiescent spectrum, and the α_{active} is calculated using the maximum flux densities at 5 and 90 GHz, illustrating the shape of the spectrum during the active state. Between 5 and 22 GHz as well as 22 and 90 GHz only the α_{active} is shown. Since exactly simultaneous data do not exist for most of the sources, we chose to use the historical maxima at each frequency to calculate the α_{active}. It is possible that the radio outburst development in reality is such that the maxima at lower frequencies are only reached after the flux is already decreasing at the higher frequencies, which means that the actual shape of the spectrum during the millimeter-wavelength activity peak is even flatter than indicated by the α_{active} index, but this practise at least prevents us from overestimating the flatness of the spectra.

As can be seen from Table 1 and from the spectral index distribution plot Fig. 1, the EGRET-detected blazars have extremely flat 5 to 90 GHz spectra especially in the active state. The median $\alpha_{5,90;active}$ during millimeter-domain activity is $\alpha = +0.02$ (for the ones that we have data for at 90 GHz). For comparison, if we only study the sources considered as "EGRET identifications with a high probability of being correct" in Mattox et al. (2001), we get the median spectral index $\alpha_{5,90;active} = +0.09$.

If all EGRET-detected AGNs have flat spectra up to the millimeter range and are variable, it is reasonable to assume that in order to be a possible counterpart for a so far unidentified EGRET source, the AGN has to have a flat radio-to-millimeter spectrum and be variable in the high-frequency radio domain.

We started by investigating the southern sources classified as potential EGRET counterparts in 3EG (marked as "a", a possible AGN, in 3EG). In this paper we study their full radio spectra and the long-term behavior at 90 and 230 GHz in order to determine if their activity in the millimeter region could confirm the identification as a blazar counterpart for the EGRET detection.

We also made high radio-frequency observations of the previously unidentified EGRET sources that could have a blazar counterpart. We study a set of sources relatively faint at 5 GHz (catalog data), and thus routinely excluded from any high radio-frequency studies, to search for AGNs with unusually flat spectra. Our assumption was that if we find objects faint at 5 GHz having a spectrum that is extremely flat or even inverted up to the millimeter-domain, these are probably sources extremely variable at millimeter wavelengths and also good candidates for gamma-ray active blazars.

4. Lower-confidence AGN identifications in 3EG

3EG lists thirteen Southern sources which are potentially identified with blazars. These sources are listed in Table 2 and their spectral index distribution is plotted in Fig. 2. The identifications are considered to be of low confidence either because the object has a low radio flux reported in the literature (historical 5 GHz flux density $S < 0.3$ Jy) or because it lies outside the 95% uncertainty contour.

If all the lower-confidence identifications with AGNs are grouped together with the high-confidence identifications and studied as "EGRET detected blazars", incorrect identifications will easily lead to incorrect conclusions about the source properties. Thus it is important to try to determine whether the possible identifications given in 3EG are correct or not.

Mattox et al. (2001) have studied the possible source identifications with an AGN in 3EG by calculating the probability of identification using the method described in Mattox et al. (1997). The method is based on using the radio fluxes at 5 GHz. The conclusion of their analysis is that 45 out of the 66 "high-confidence AGN identifications" in 3EG have a high probability of being correct and 20 of them are plausible. Of the 27 "lower-confidence identifications" in 3EG they only find one to be robust, three to be plausible, and 23 unlikely.

There are several problems with trying to identify a promising AGN counterpart using low-frequency radio data from published catalogs. The 5 GHz catalog data used for the 3EG source identifications of the Southern sources (Wright et al. 1994; Griffith et al. 1994, 1995) are from 1990, i.e. nonsimultaneous with the EGRET observations. As mentioned in Section 3, there is plenty of evidence that the gamma-ray activity of AGNs correlates with the millimeter-domain activity. Many AGNs, however, are known to be highly variable in the radio/mm domain, and thus the historical one-epoch low-frequency fluxes can not be expected to correlate well with the millimeter-fluxes during the time of the EGRET observations.

Also, there are several AGNs with radio spectra that are inverted up to the millimeter-domain at least during their active state (Tornikoski et al. 2000b, 2001), so the low-frequency fluxes in general do not give an accurate estimate of the millimeter-wavelength brightness of these sources.

In order to study the lower-confidence AGN identifications in 3EG we used millimeter-data from our group's SEST observations (90 and 230 GHz), complemented with data from the literature, as described in Section 2. For most of the sources we have relatively long data sets which gives us a good estimate of their flux history and the overall variability behavior, and for some sources we had data taken (semi-)simultaneously with EGRET. We also studied the complete radio continuum spectra of these sources. Even most of the 5 GHz fluxes from Tornikoski et al. (1993), Bramwell 1993 (private communication), Reich et al. (1998) and Reich et al. (2000) are newer than the catalog data used by Mattox et al. (2001).

We have made SEST observations for 12 of the 13 Southern Hemisphere sources classified as lower-confidence identifications with AGNs in 3EG, and we discuss them here individually. The source B1920−211 (J1923−2104), given as a potential counterpart for 3EG J1921-2015 in 3EG and considered "a plausible EGRET identification" in Mattox et al. (2001) has not been observed by our group.

The radio spectra of these twelve sources are shown in Figs. 3–4, and the flux density curves of the sources for which we have time variability data are shown in Figs. 5–13. In the following, the abbreviation BLO stands for a BL Lacertae Object, LPQ for a Low Polarization Quasar with a measured optical polarization $p < 3\%$, HPQ for a Highly Polarized Quasar with a measured optical polarization $p > 3\%$, and QSO for a quasar with no polarization information available.

B0130−171, a possible counterpart for 3EG J0130−1758 (z=1.020, QSO, Fig. 3 panel a.) A quasar for which there are only two 90 GHz data points taken more than

14 years apart, and no 230 GHz data points. The difference between the flux densities of these two 90 GHz points shows that the source can be extremely variable. With the more recent data point the radio spectrum becomes inverted up to the millimeter-domain (with $\alpha_{5,90;active} = +0.20$). We consider B0130−171 a likely counterpart for 3EG J0130−1758.

B0506−612, a possible counterpart for 3EG J0512−6150 (z=1.093, LPQ, Fig. 3 panel b and Fig.5.) The radio flux curves, even though sparsely sampled, show no signs of any prominent activity and the flux levels remain relatively low (ca. 1–1.5 Jy at 90 GHz, ca. 0.5 Jy at 230 GHz), also at the time of the EGRET detections. The radio spectrum is relatively flat ($\alpha_{5,90;active} = -0.13$) but the spectral index remains almost constant from the minima to the maxima.

B0521−365, a possible counterpart for 3EG J0530−3626 (z=0.061, BLO, Fig. 3 panel c and Fig. 6.) This BL Lacertae Object has been monitored with the SEST frequently before and during the Compton mission, and it shows relatively high flux levels (over 5 Jy at 90 GHz) and complex variability. The EGRET detections with $(TS)^{1/2} \geq 2$ were made close to the increased activity at the high radio frequencies. The radio spectrum of this source is steep in the quiet state: $\alpha < -0.50$ all the way from very low radio frequencies to the millimeter-domain, and even in the active state the radio spectrum does not flatten considerably ($\alpha_{5,90;active} = -0.21$), i.e. remains steeper than for typical EGRET-detected blazars in spite of the variability.

B0537−286, a possible counterpart for 3EG J0531−2940 (z=3.104, LPQ, Figs. 3 panel d and Fig. 7.) A very high-redshift quasar for which there is only little radio data. The radio spectrum is inverted up to 10 GHz in the active state, but becomes steeper after that and remains very faint in the millimeter-domain ($S_{230} < 0.2$ Jy, $S_{90} < 0.6$ Jy), also during the EGRET pointings. The lack of activity at the high frequencies and the steepness of the high-frequency part of the radio spectrum ($\alpha_{5,90}$ ranging from -0.32 to -0.20) suggest that this source is not a likely counterpart for 3EG J0531−2940.

B0539−057, a possible counterpart for 3EG J0542−0655 (z=0.839, QSO, Fig. 3 panel e and Fig. 8.) A quasar which has always been faint at 90 GHz, and below the detection limit at 230 GHz (with an 4σ upper limit $S_{230} \approx 250$ mJy). The high-frequency part of the radio spectrum is steep, with $\alpha_{5,90} \approx -0.40$. The low activity in the millimeter region and the steep radio spectrum suggest that B0539−057 is not the likely counterpart of 3EG J0542−0655.

B0805−077, a possible counterpart for 3EG J0812−0646 (z=1.837, QSO, Fig. 3 panel f and Fig. 9.) For this source there are only few EGRET data points. The 90 GHz flux level has remained relatively constant ($S_{90} < 1.5$ Jy) from 1987 to 1994, also during the EGRET pointings, even though moderate increase in the millimeter-fluxes can be seen at the time of the EGRET detections. The 90 GHz flux, however, shows a prominent increase ($S_{90} = 2.5$ Jy) in the beginning of 1997, after which we unfortunately have no further data. The radio spectrum is flat ($\alpha_{5,90} = -0.07$) up to 100 GHz in the quiet state, and becomes extremely inverted ($\alpha_{5,90} = +0.30$) in the active state. The flat to inverted high-frequency part of the radio spectrum indicates considerable millimeter-wavelength activity in this source, and we consider it a likely counterpart for 3EG J0812−0646.

B1127−145, a possible counterpart for 3EG J1134−1530 (z=1.187, LPQ, Fig. 4 panel a and Fig. 10.) The increase in the EGRET fluxes in the beginning of 1993 and 1995 coincide with increased activity in the millimeter-domain, but the high-frequency part of the radio spectrum remains steep even during the active state ($\alpha_{5,90;active} = -0.33$). This source, however, is bright and variable all the way from the low-frequency to the millimeter-domain, with the maximum flux densities at 90 GHz and 230 GHz being 2.15 Jy and 1.30 Jy, respectively. In spite of the somewhat steep high-frequency part of the radio spectrum we consider this source a possible EGRET counterpart.

B1313−333, a possible counterpart for 3EG J1314−3431 (z=1.210, QSO, Fig. 4 panel b and Fig. 11.) This source is very variable at the high radio-frequencies. The EGRET detections with $(TS)^{1/2} \geq 2$ have been made at the increase of millimeter-wavelength activity, from the end of 1991 to the first half of 1993. The radio spectrum of B1313−333 is extremely flat, ranging from $\alpha_{5,90} = -0.13$ in the quiet state to $\alpha_{5,90} = +0.27$ in the active state. We consider B1313−333 a likely counterpart for 3EG J1314−3431.

B1504−166, a possible counterpart for 3EG J1504−1537 (z=0.876, HPQ, Fig. 4 panel c and Fig. 12.) This source has only one significant EGRET detection. An increase in the radio flux levels coincides with the time of the EGRET detection, even though no major radio outbursts are seen during that time. The radio spectrum is flat between 1 and 30 GHz and then becomes steeper, with $\alpha_{5,90} = -0.44$ in the quiet state to $\alpha_{5,90} = -0.26$ in the high state.

B1514−241 (AP Lib), a possible counterpart for 3EG J1517−2538 (z=0.049, BLO, Fig. 4 panel d and Fig. 13.) A BL Lacertae object for which we have relatively long and densely sampled millimeter flux curves that show increased activity at the time of the increase in the EGRET fluxes (in 1992.2 and 1993.7–1994.8). The radio spectrum is very flat, ranging from $\alpha_{5,90} = -0.16$ in the quiet state to $\alpha_{5,90} = +0.11$ in the active state. We consider B1514−241 a very likely counterpart for 3EG J1517−2538. This object was also the only source studied in our set of 12 sources that Mattox et al. (2001) list as "EGRET identifications with a high probability of being correct".

B1716−771, a possible counterpart for 3EG J1720−7820, and J1808−501, a possible counterpart for 3EG J1806−5005 For each of these two sources, both at an unknown redshift, we only have one 90 GHz data point, taken after the end of EGRET operation. For both of them the S/N of the 90 GHz observation was less than 4, giving us only the upper limit of the source flux density (with the 4σ upper limit of $S_{90} < 370$ mJy for B1716−771 and $S_{90} < 250$ mJy for J1808−501). Since both of these sources were faint at the time of the 90 GHz observation, they are neither very promising candidates for strong millimeter-wave activity nor very good candidates for the EGRET-detection counterparts.

5. Millimeter-domain observations of promising candidates for new Southern EGRET identifications

As mentioned in Section 4, Mattox et al. (1997), hereafter MSM, have presented a method to make new identifications for the unidentified sources listed in the 2nd EGRET catalog (Thompson et al. 1995), hereafter 2EG, and the Supplement to the 2nd EGRET catalog (Thompson et al. 1996), hereafter 2EGS. MSM list 17 potential identifications for which they expect further investigation to be most useful.

When we exclude all Northern Hemisphere sources and all the sources that have been either left out from 3EG (after the improved analysis), or identified in the 3EG (including the two sources identified using our group's observations in Bloom et al. (1997)), this leaves us with two sources: J1249−8303 and J1650−5044, Table 3. The table lists the observed AGN counterpart, the possible EGRET catalog identification, the epoch of the 90 GHz observation, the flux density at 90 GHz for the source that was detected at a significant (signal-to-noise $\geq$4.0) level, and the spectral index between 5 and 90 GHz.

The first of the two "promising candidates" from MSM, J1249−8303, was not detected at a significant level at 90 GHz (the 4σ upper limit of S_{90} being 308 mJy). The second source, J1650−5044, has a millimeter flux and spectrum which would make it a very promising candidate for the AGN counterpart of the EGRET detection, but in 3EG Hartman et al.

comment that the corresponding 3EG source, 3EG J1638−5155, lies 2° away from the 2EG position, and that the possible identification by MSM of 2EG J1648−5042 with this AGN thus appears less convincing.

MSM list radio sources as potential source identifications for the 2EG and the 2EGS with the probabilities of correct identification, based on the radio source position and flux density. The sources with the highest probabilities have been identified with the 2EG/2EGS sources either in the same paper (Table 3 of MSM, "EGRET identifications with a high probability of being correct") or later in 3EG. The probability listed in MSM is, however, based on low frequency radio fluxes of the Parkes-MIT-NRAO survey (Griffith & Wright 1993), hereafter PMN, obtained in 1990 at 4.8 GHz. We have composed a list of candidates for radio identifications of EGRET sources from MSM Tables 1 and 2, excluding all Northern Hemisphere sources, all sources that have been identified in MSM, or in Bloom et al. (1997), or in 3EG, and all that have the identification probability $p < 0.001$.

There were 20 sources left in our sample, and we managed to observe 19 of them, shown in Table 4. The columns are as in Table 3, except that the flux density column shows "N.D." ("no detection") for sources with a signal-to-noise (S/N) ratio <2.0, and the marginal detections, with $2.0 < S/N < 4.0$, have an S/N entry included in the flux density column. All other data points have S/N $\geq$ 4.0 and are considered detections at a significant level. The flux limit for a S/N ≥ 4 detections under these observing conditions was approximately 350 mJy. The integration times chosen for most of these sources were 14 $\times$ 25 s for each beam in the dual beam switching mode, optimized for sources that would be in the order of $S_{90} \geq 0.5$ Jy, i.e. "brighter than expected".

Three of the sources (J0726−4728, J1058−8003, J1703−6212) with a significant ($S/N > 4$) detection at 90 GHz have a flat 5 to 90 GHz spectrum, which make them good candidates for the counterparts of the EGRET detections. J1058−8003 and J1703−6212 have a 90 GHz flux density $S_{90} > 1$ Jy in this one-epoch data set, showing that these sources can be bright in the millimeter-domain, and having a flat spectrum up to the 100 GHz region they are probably variable sources with blazar-like characteristics in the millimeter-domain.

In addition to the aforementioned objects, there are two sources (J1454−1925 and J2005−2310) with a marginal 90 GHz detection and a relatively flat spectrum. It is worth making further millimeter-wave observations of these sources at some other epochs to see whether their high radio-frequency variability corresponds to that of other flat-spectrum sources and thus makes them possible candidates for the EGRET identifications.

6. Possible candidates for new Southern 3EG EGRET identifications

In order to try to identify AGN counterparts for 3EG sources with no identifications in the catalog, we chose potential new counterpart candidates according to the following criteria:

- Only Southern Hemisphere sources with $|b| > 10°$ were included.
- Only sources with no entry in 2EG or 2EGS were included, i.e., these are new sources not earlier discussed by MSM, and also these were more likely to be in an active radio state during our observations in 2000 if compared to "old" EGRET detections from 2EG.
- We searched for the candidates within a 1° radius of the 3EG position, which is the size of the EGRET error box.
- In the first stage we selected candidates which are radio sources from the PMN survey or the Parkes survey (Wright & Otrupcek 1990), hereafter PKS. There were several candidates for each 3EG source.
- From the candidates we excluded all of those that had a 5 GHz flux in the PMN survey less than 200 mJy. Even though the PMN fluxes are one-epoch fluxes obtained almost 10 years earlier of sources which are expected to be highly variable, it is reasonable to assume that very few if any of the extremely faint sources would be detected in the millimeter-domain with the current sensitivity of the SEST instruments.

We observed 19 of the EGRET source counterpart candidates at 90 GHz in April 2000 and/or August 2000. They are shown in Table 5. Among these sources there are two significant detections ($S/N \geq 4.0$) at 90 GHz. One of them, J1819−6345, is a known compact steep-spectrum source, and our 90 GHz data point confirms the steepness of its spectrum. It is an unlikely AGN counterpart for an EGRET-detection.

J1605−1139 has a flux density of 530 mJy at 90 GHz and a 5 to 90 GHz spectral index $\alpha = +0.12$, making it a good candidate for millimeter-range activity. This source is located within $50.6'$ of the EGRET position of 3EG J1607−1101.

There were three other flat-spectrum ($\alpha > -0.20$) sources (J0710−3850, J1254−4425 and J2249−1251) detected at a marginal level at 90 GHz. Since our study of this sample was made using 1–2 observing epochs only, the millimeter-variability behavior of these sources is currently unknown, but the flatness of their spectra indicates that they could be active also at the higher radio frequencies.

Because all the sources studied in this sample were observed *after* the EGRET was operational, it is impossible to estimate what the millimeter flux densities were *during* the EGRET detections, and we can only conclude that the sources that were now detected at a significant level can at least sometimes be bright at 90 GHz.

7. Conclusions

We have studied high radio-frequency (90 and 230 GHz) data of southern AGNs that are possible counterparts for the sources listed in the Third EGRET Catalog.

The high-confidence AGN identifications in 3EG are objects that are bright and variable in the millimeter-domain, having a flat spectrum up to $\nu \approx 100$ GHz, and in our search for EGRET source counterparts we tried to find sources that have flat spectra and show millimeter-wavelength activity, preferably close to the time of the EGRET detection.

We first studied the sample of Southern sources classified as "possible AGN identifications" in 3EG. We have millimeter-wavelength data for 12 of them (out of 13), ranging from one-epoch observations to more than 65 data points at 90 GHz from a period of more than 13 years. The objects B0130−171, B0805−077, B1313−333 and B1514−241 were found to have extremely flat spectra (inverted up to 100 GHz in the active state) and to be bright and variable in the millimeter-domain (with $S_{90,max}$ ranging from 1.76 Jy to 3.13 Jy), thus confirming the identification. B1127−145 has a somewhat steeper spectrum but can still be the correct identification. For some of the aforementioned sources we have data that show that the gamma-detection was made at the time of increased activity at high radio-frequencies.

The objects B0537−286, B0539−057, B1716−771 and J1808−5011 have steeper spectra ($\alpha_{5,90} < -0.20$ even in the active state) and all are faint at high radio-frequencies (with the largest $S_{90,max}$ =580 mJy) . We do not consider them likely counterparts of the 3EG sources.

The remaining objects, B0506−612, B0521−365 and B1504−166 are all relatively bright and active in the millimeter-domain and even though they show blazar-like characteristics and could be the correct identifications for the 3EG counterparts, they lack some features of the aforementioned convincing cases.

We have also studied the millimeter flux densities and the 5 to 90 GHz spectra of sources that were considered possible identifications for the so far unidentified EGRET sources. We suggest that the following four EGRET sources can possibly be identified with an AGN: 2EG 0720−4746 (id: J0726−4728), 2EGS 1050−7650 (id: J1058−8003), 2EGS 1703−6302 (id: J1703−6212), and 3EG J1607−1101 (id: J1605−1139). In addition to these, we found that five other AGNs, though faint at 90 GHz, seem to have flat 5 to 90 GHz spectra, which indicates millimeter-activity that may be related to the gamma-ray activity.

We acknowledge the support of the Academy of Finland for this work. The SEST is operated jointly by ESO and the Swedish National Facility for Radio Astronomy, Onsala Space Observatory at Chalmers University of Technology. This research has made use of the SIMBAD database, operated at CDS, Strasbourg, France, and the NASA/IPAC Extragalactic Database (NED) which is operated by the Jet Propulsion Laboratory, California Institute of Technology, under contract with the National Aeronautics and Space Administration.

REFERENCES

Beasley, A. J., Conway, J. E., Booth, R. S., Nyman, L.-A., & Holdaway, M. 1997, A&AS, 124, 469

Bloom, S. D., Hartman, R. C., Teraesranta, H., Tornikoski, M. & Valtaoja, E. 1997, ApJ, 488, L23

Bondi, M., Padrielli, L., Fanti, R., Ficarra, A., Gregorini, L. & Mantovani, F. 1996, A&AS, 120, 89

Bramwell, D. 1993, private communication

Combi, J. A., Romero, G. E., Benaglia, P. 1999, AJ, 118, 659

Drinkwater M. J. et al. 1997, MNRAS, 284, 85

Ghosh, T., Gopal-Krishna, Rao, A. P. 1994, A&AS, 106, 29

Griffith & Wright 1993, AJ, 105, 1666

Griffith, M. R., Wright, A. E., Burke, B. F. & Ekers, R. D. 1994, ApJS, 90, 179

Griffith, M. R., Wright, A. E., Burke, B. F. & Ekers, R. D. 1995, ApJS, 97, 347

Fichtel, C. E. et al. 1994 ApJS, 94, 551

Hartman et al. 1999, ApJS, 123, 79 (3EG)

Kovalev Y. Y., Nizhelsky, N. A., Kovalev, Yu. A., Berlin, A. B., Zhekanis, G. V., Mingaliev, M. G., Bogdantsov, A. V. 1999, A&AS, 139, 545

Kuehr, H., Witzel, A., Pauliny-Toth, I. I. K. & Nauber, U. 1981, A&AS, 45, 367

Large, M. I., Cram, L. E., Burgess, A. M. 1991, Obs, 111, 72

Lawrence, C. R., Bennett, C. L., Garcia-Barreto, J. A., Greenfield, P. E. & Burke, B. F. 1983, ApJS, 51, 67

Lähteenmäki, A., Teräsranta, H., Wiik, K. & Valtaoja, E. 1997, in Proc. 4th Compton Symposium, eds. C. D. Dermer, M. Strickman & J. D. Kurfess (New York, AIP), p.1452.

Lähteenmäki, A., Valtaoja, E. & Tornikoski, M. 2000, in Proc. 5th Compton Symposium, eds. M. L. McConnell & J. M. Ryan (New York AIP), p. 372

Lähteenmäki, A. & Valtaoja, E. 2001, in Proc. Gamma 2001 Symposium, eds. S. Ritz, N. Gehrels & C. R. Shrader (New York AIP), p. 301

Mattox, J. R., Schachter, J., Molnar, L., Hartman, R. C. & Patnaik, A. R. 1997, ApJ, 481, 95 (MSM)

Mattox, J. R., Hartman, R. C. & Reimer, O. 2001, ApJS, 135, 155

Punsly, B. 1997, AJ, 114, 544

Reich, W., Reich, P., Pohl, M., Kothes, R. & Schlickeiser, R. 1998, A&AS, 131, 11

Reich, W., Fuerst, E., Reich, P., Kothes, R., Brinkmann, W. & Siebert, J. 2000, A&A, 363, 141

Reuter, H.-P. et al. 1997, A&AS, 122, 271

Salonen, E. et al. 1987, A&AS, 70, 409

Steppe, H., Salter, C. J., Chini, R., Kreysa, E., Brunswig, W., Lobato Perez, J. 1988, A&AS, 75, 317

Steppe, H. et al. 1992, A&AS, 96, 441

Steppe, H. et al. 1993, A&AS, 102, 611

Teräsranta, H. et al. 1987, A&AS, 71, 125

Teräsranta, H. et al. 1992, A&AS, 94, 121

Teräsranta, H. et al. 1998, A&AS, 132, 305

Teräsranta, H., Urpo, S., Wiren, S. & Valtonen, M. 2001, A&A, 368, 431

Thompson, D. J., et al. 1995, ApJS, 101, 259 (2EG)

Thompson, D. J. et al. 1996, ApJS, 107, 227 (2EGS)

Tornikoski, M., Valtaoja, E., Teräsranta, H., Lainela M., Bramwell, D. & Botti, L. C. L. 1993, A&A, 289, 673

Tornikoski, M., Valtaoja, E., Teräsranta, H., Smith, A. G., Nair, A. D., Clements, S. D. & Leacock, R. J. 1994, A&A, 289, 673

Tornikoski, M. et al. 1996, A&AS, 116, 157

Tornikoski, M. et al. 1999, AJ, 118, 1161

Tornikoski, M. & Lähteenmäki, A. 2000a, in Proc. 5th Compton Symposium, eds. M. L. McConnell & J. M. Ryan (New York AIP), p. 372

Tornikoski M., Lainela, M., Valtaoja, E. 2000b, AJ, 120, 2278

Tornikoski M., Jussila, I., Johansson, P., Lainela, M. & Valtaoja, E. 2001, AJ, 121, 1306

Valtaoja, E. & Teräsranta, H. 1996, A&AS, 120, 491

Wright & Otrupcek 1990, Parkes Radio Sources Catalogue, Version 1.01, Australia Telescope National Facility, Parkes

Wright, A. E., Wark, R. M., Troup, E., Otrupcek, R., Jennings, D., Hunt, A. & Cooke, D. J. 1991, MNRAS, 251, 330

Wright, A. E., Griffith, M. R., Burke, B. F. & Ekers, R. D. 1994, ApJS, 91, 111

Zook, Z. C., Giammona, W. J., Unwin, S. C. 1997, AJ, 114. 1121

This preprint was prepared with the AAS LaTeX macros v5.0.

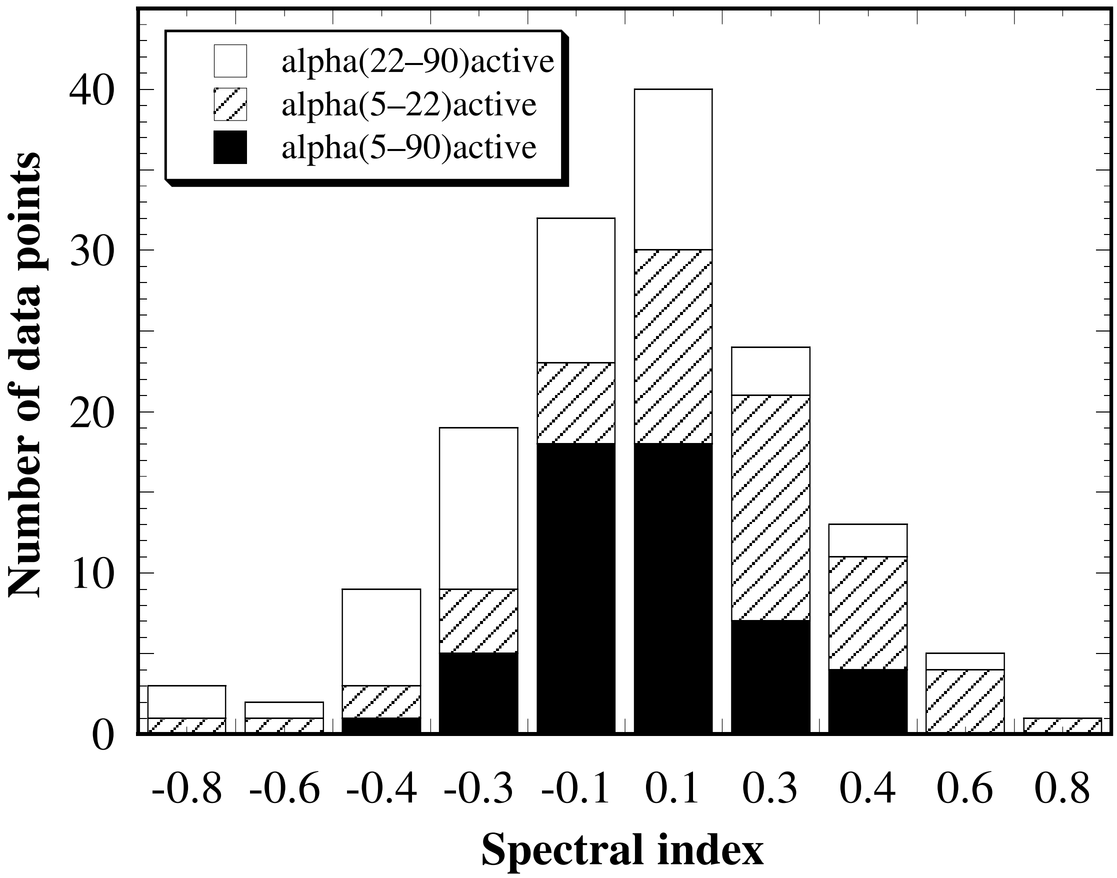

Fig. 1.— Spectral index distribution of the sources in Table 1 (3EG high-confidence identifications with AGNs).

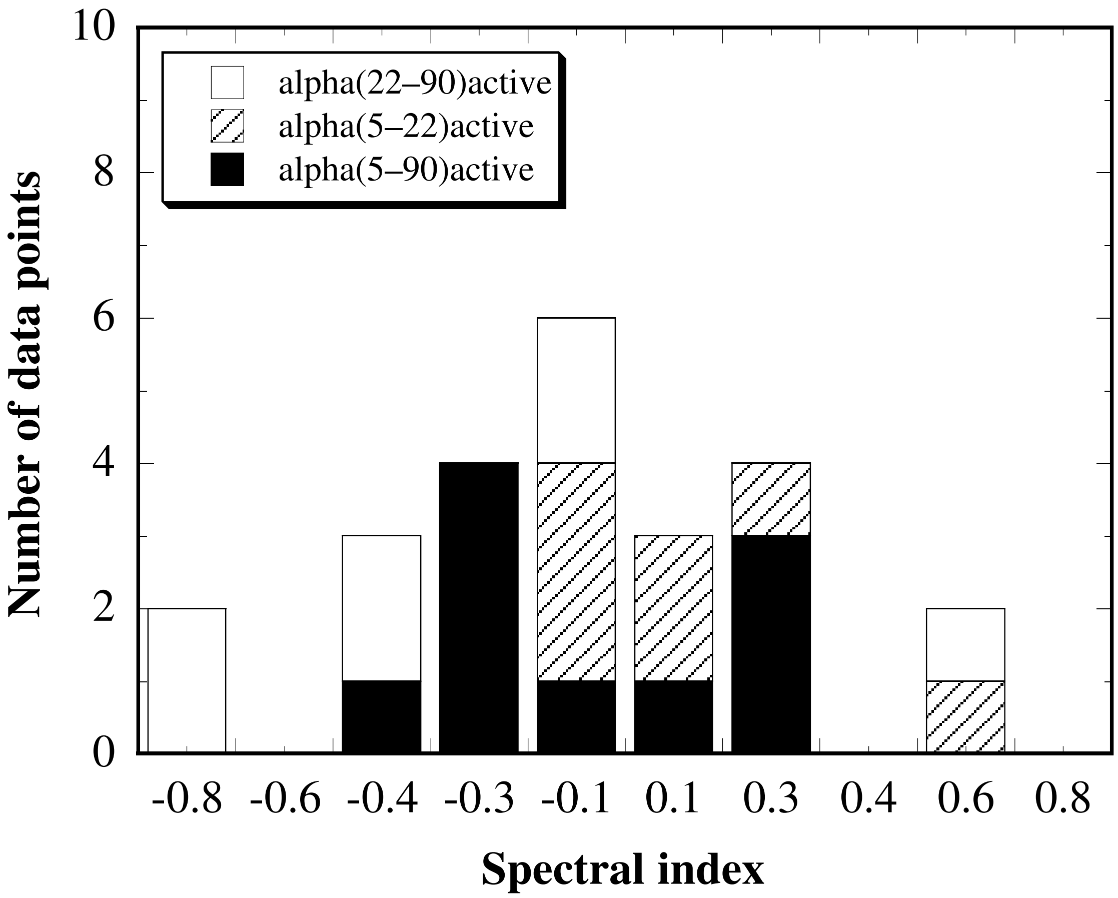

Fig. 2.— Spectral index distribution of the sources in Table 2 (3EG lower-confidence identifications with Southern AGNs).

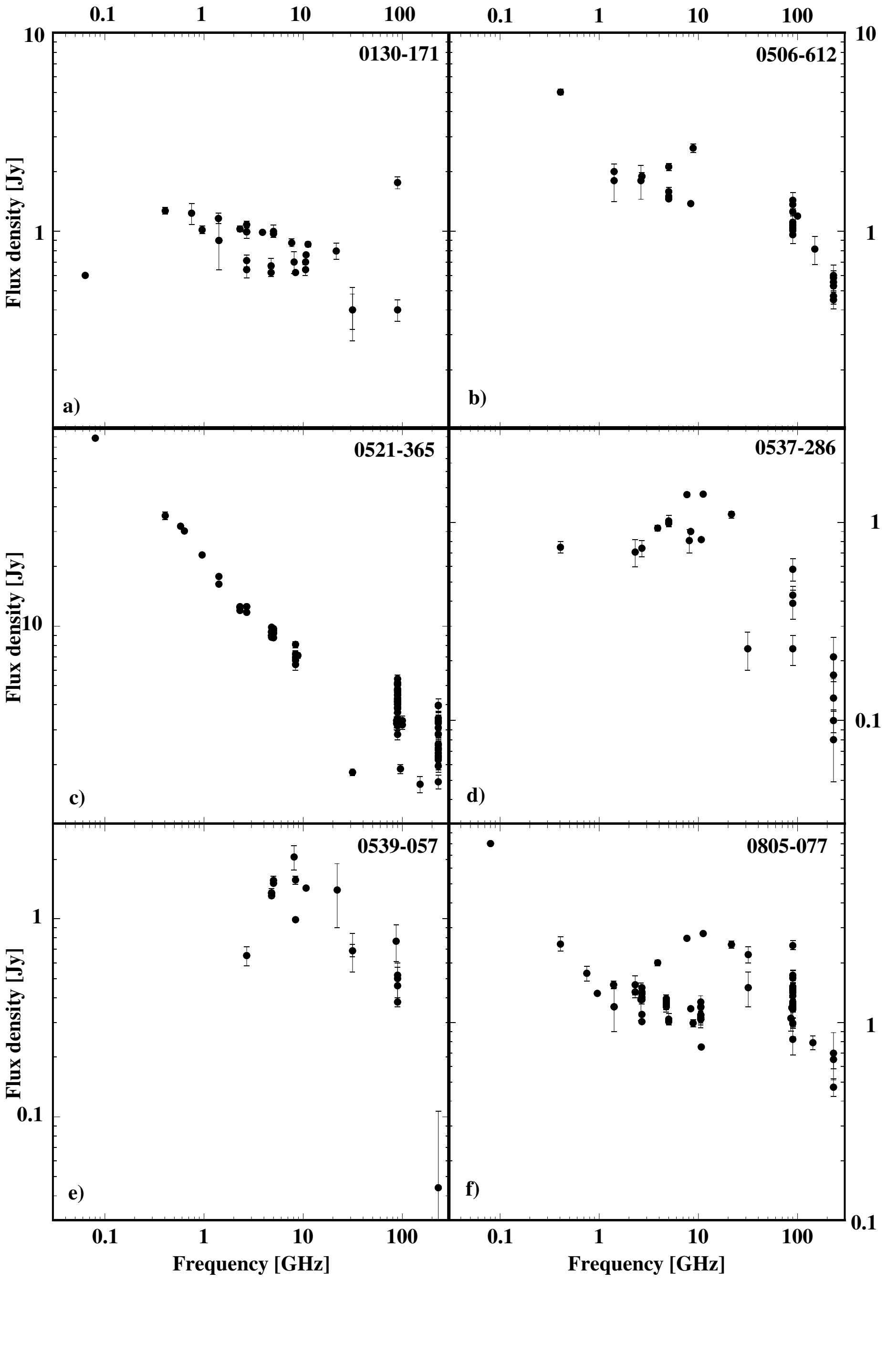

Fig. 3.— Radio spectra of AGNs that are lower-confidence identifications of the EGRET sources in 3EG: (a) B0130−171, (b) B0506−612, (c) B0521−365, (d) B0537−286, (e) B0539−057, (f) B0805−077.

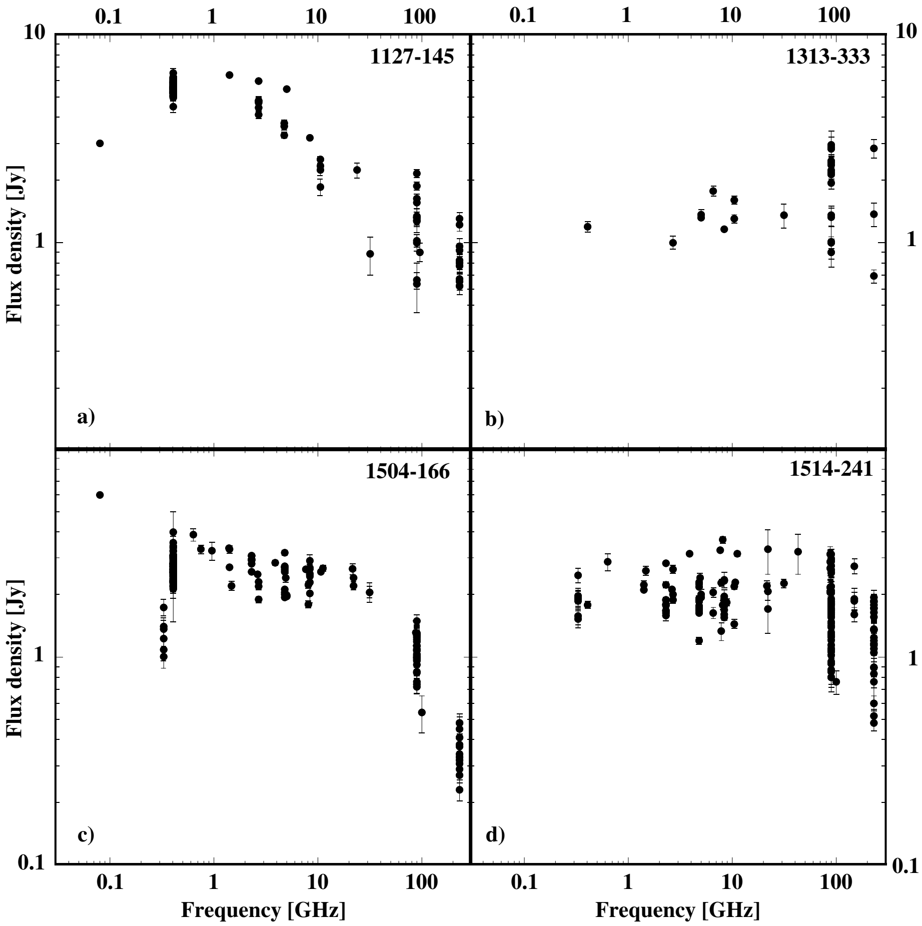

Fig. 4.— Radio spectra of AGNs that are lower-confidence identifications of the EGRET sources in 3EG: (a) B1127−145, (b) B1313−333, (c) B1504−166, (d) B1514−241.

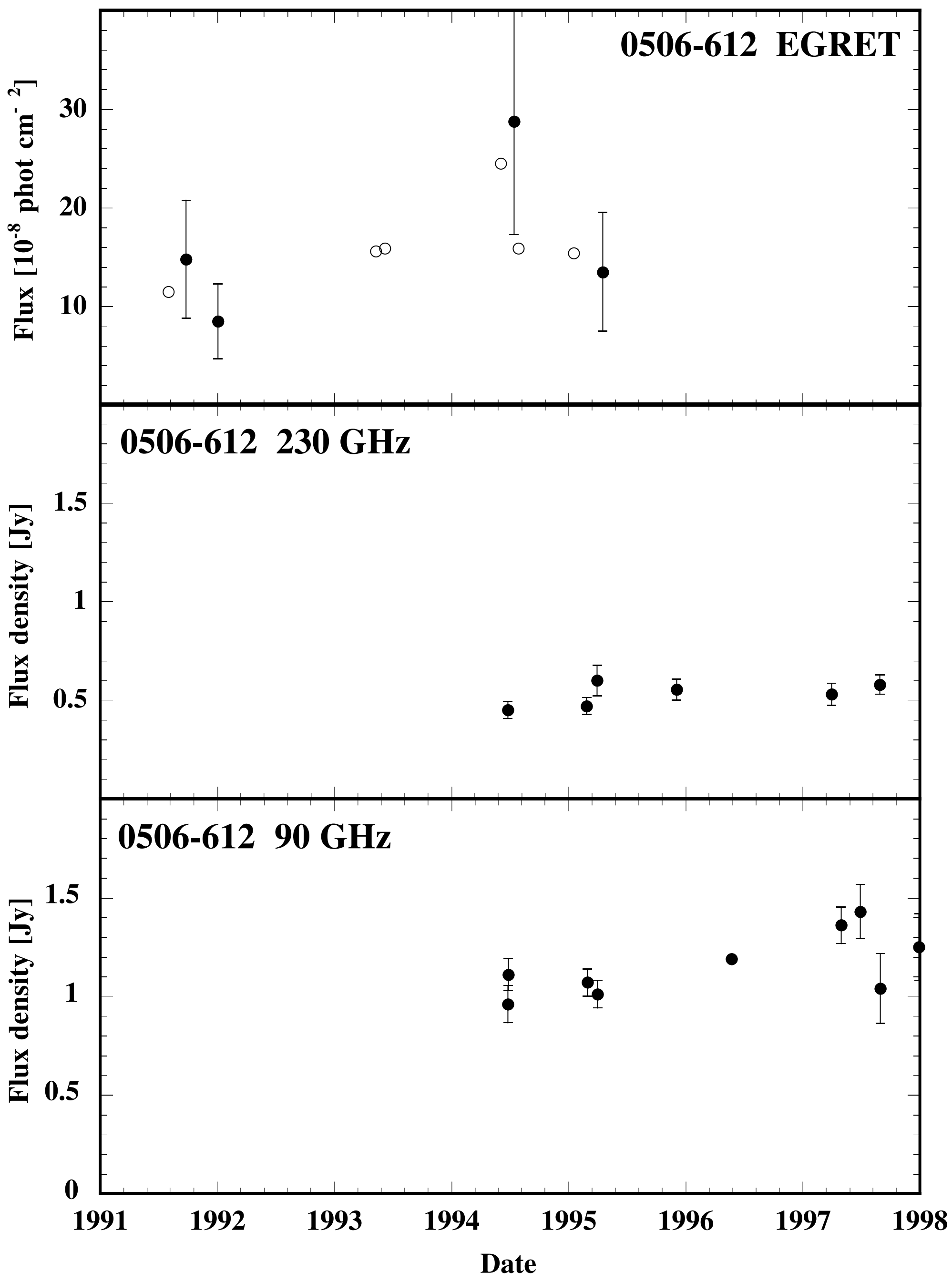

Fig. 5.— Flux density curves for B0506−612. The top panel shows the EGRET observations with $(TS)^{1/2} \geq 2$ with error bars, filled circles, and the EGRET upper limits with $(TS)^{1/2} < 2$, open circles. The 230 GHz flux curve is shown in the middle, and the 90 GHz flux curve at the bottom.

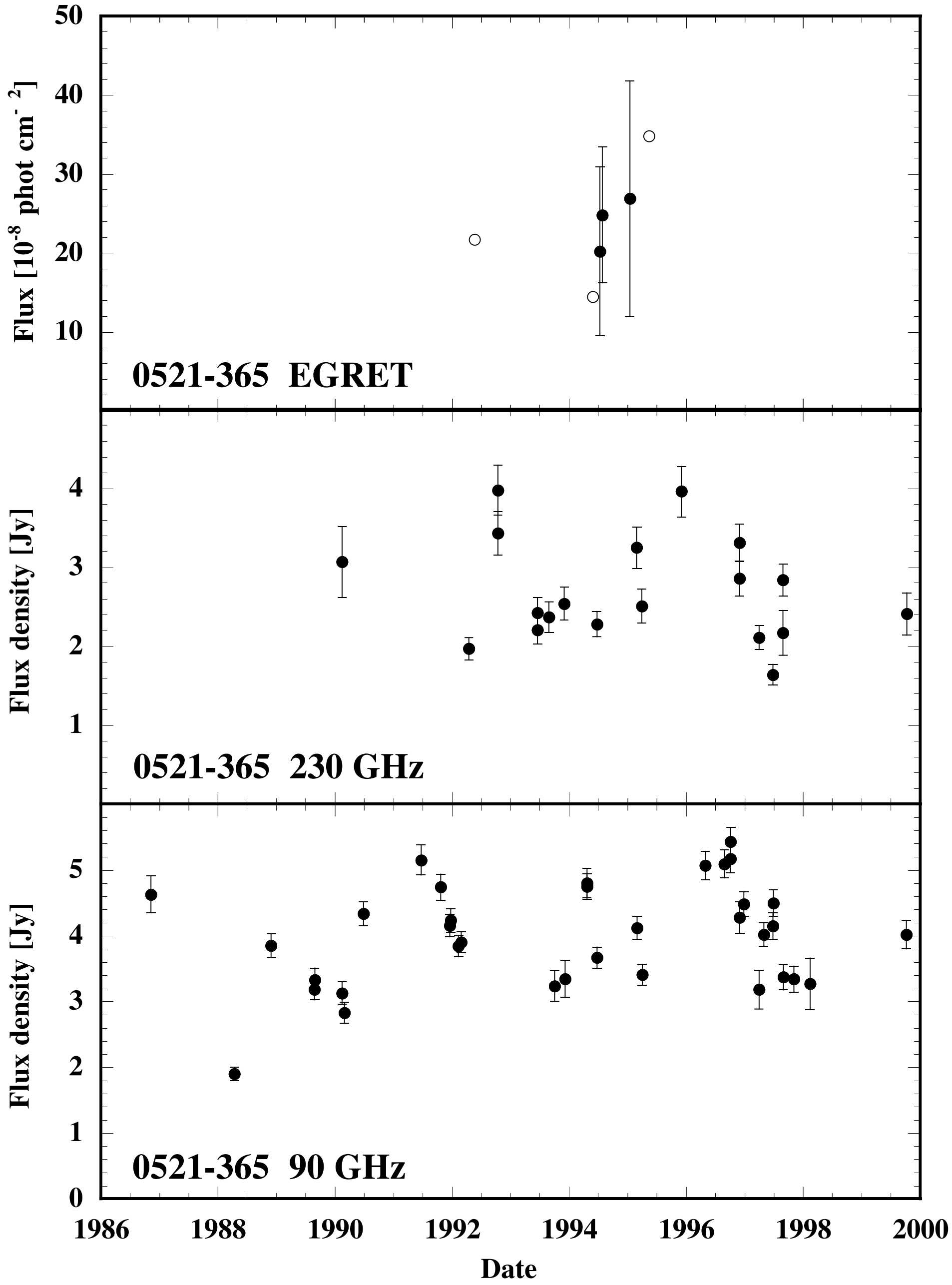

Fig. 6.— As Fig. 5 but for the source B0521−365.

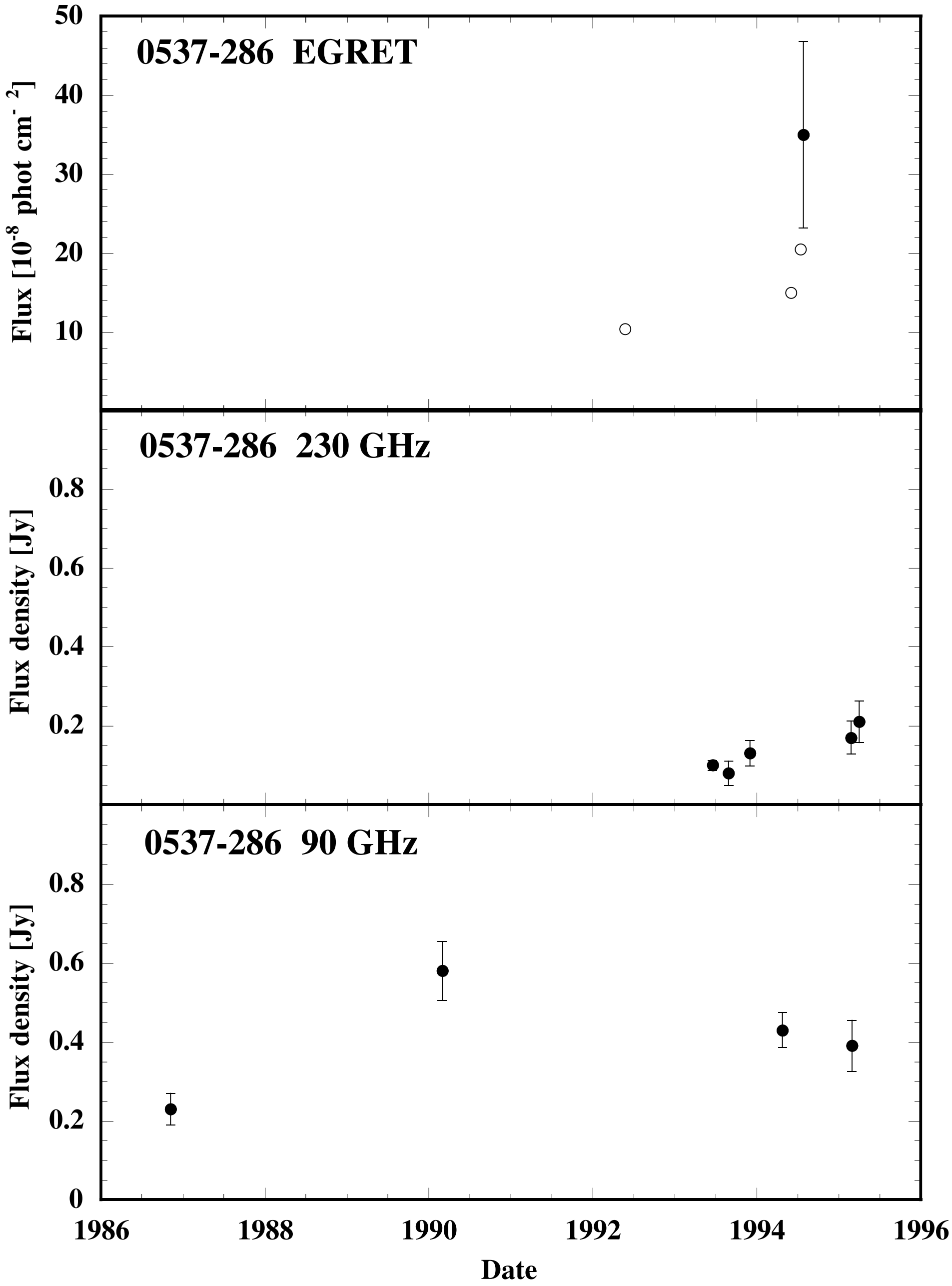

Fig. 7.— As Fig. 5 but for the source B0537−286.

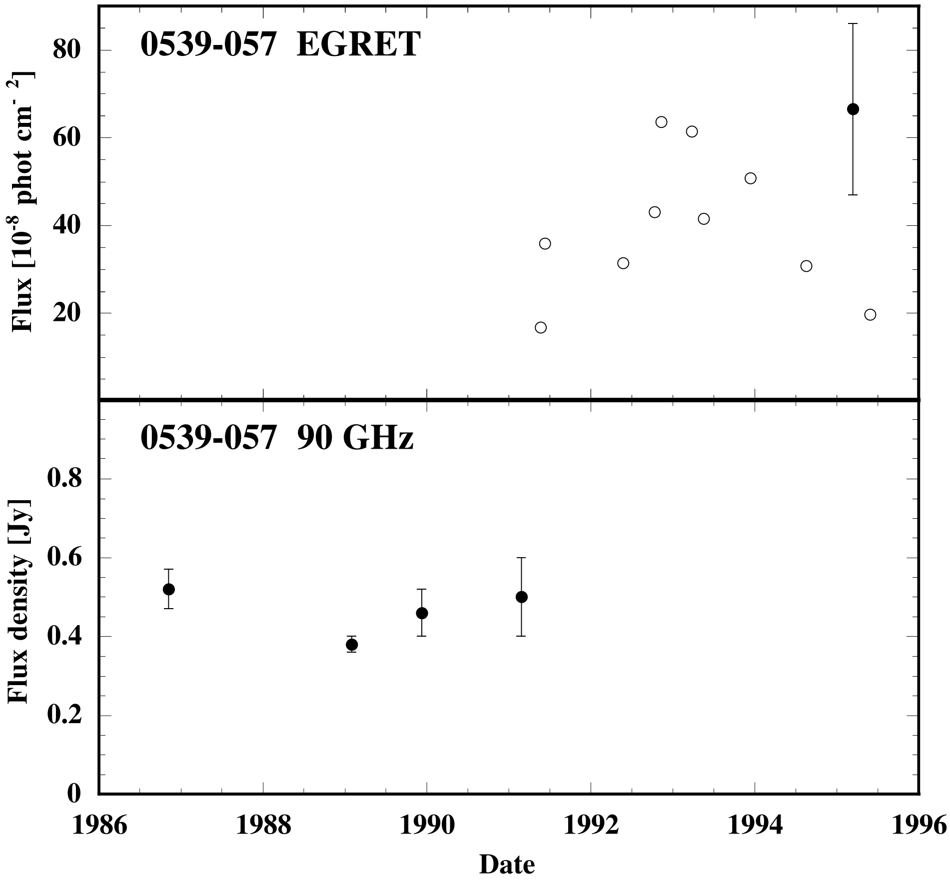

Fig. 8.— As Fig. 5 but for the source B0539−057, and only the EGRET data and 90 GHz radio data were available.

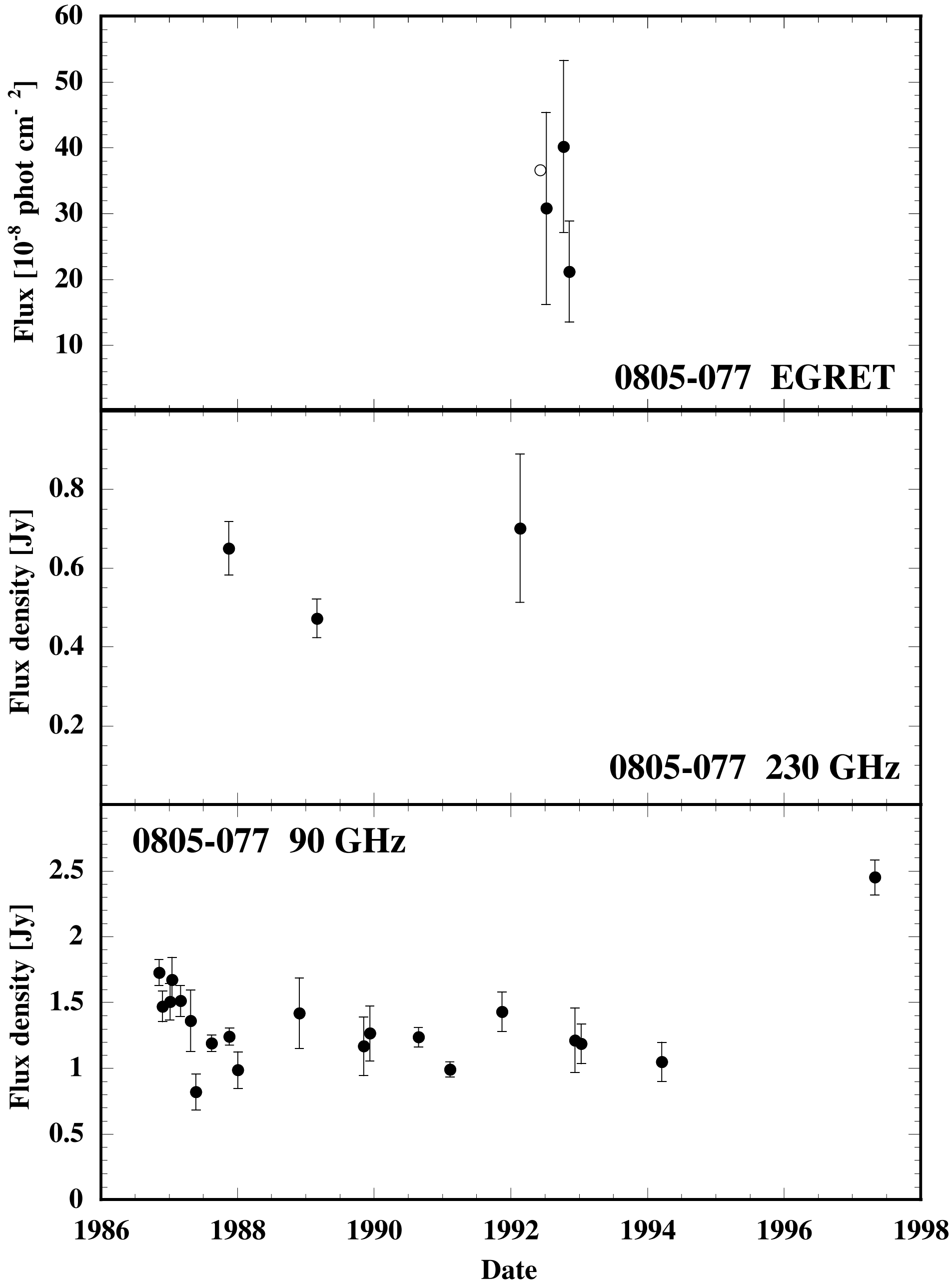

Fig. 9.— As Fig. 5 but for the source B0805−077

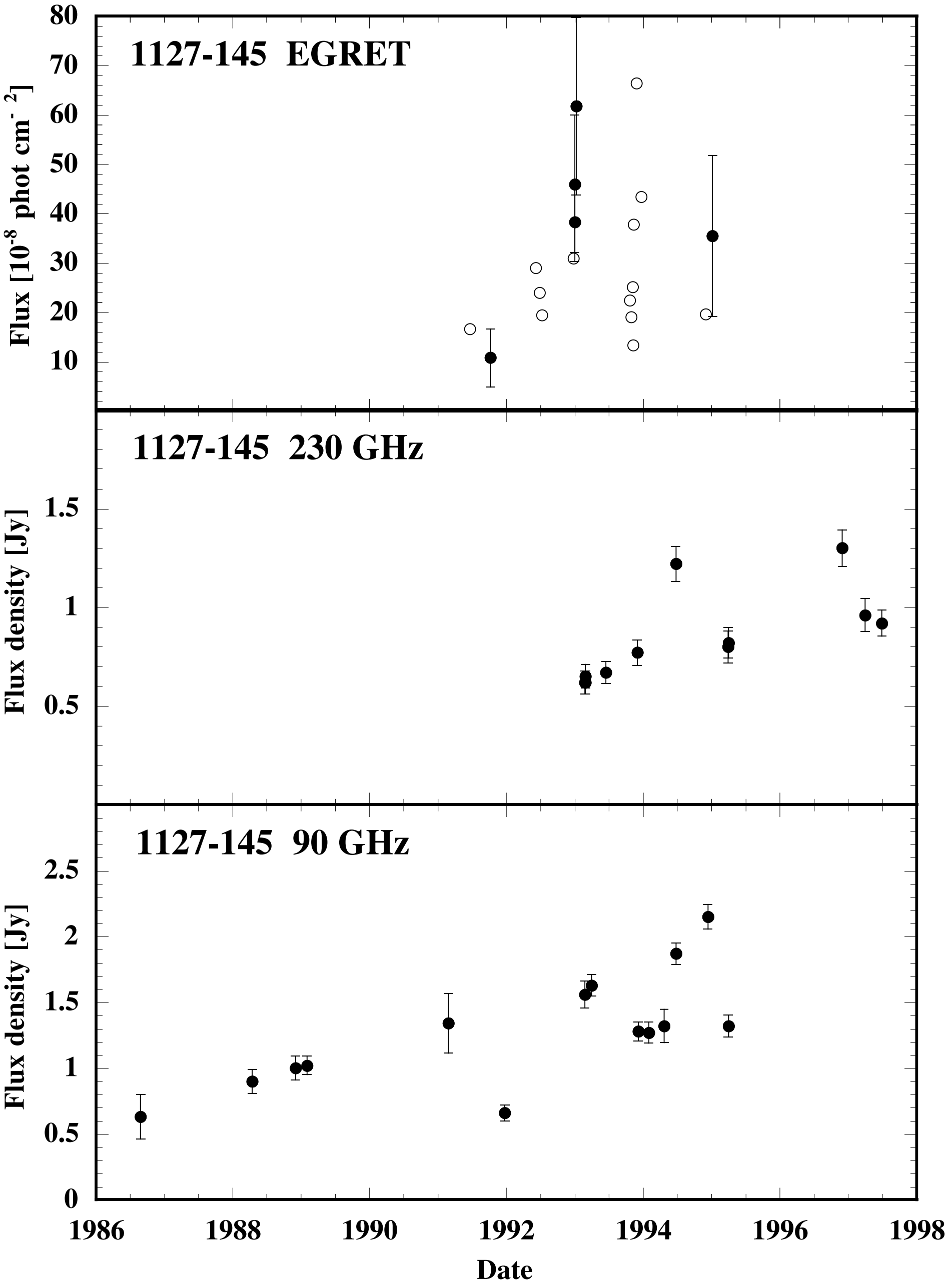

Fig. 10.— As Fig. 5 but for the source B1127−145.

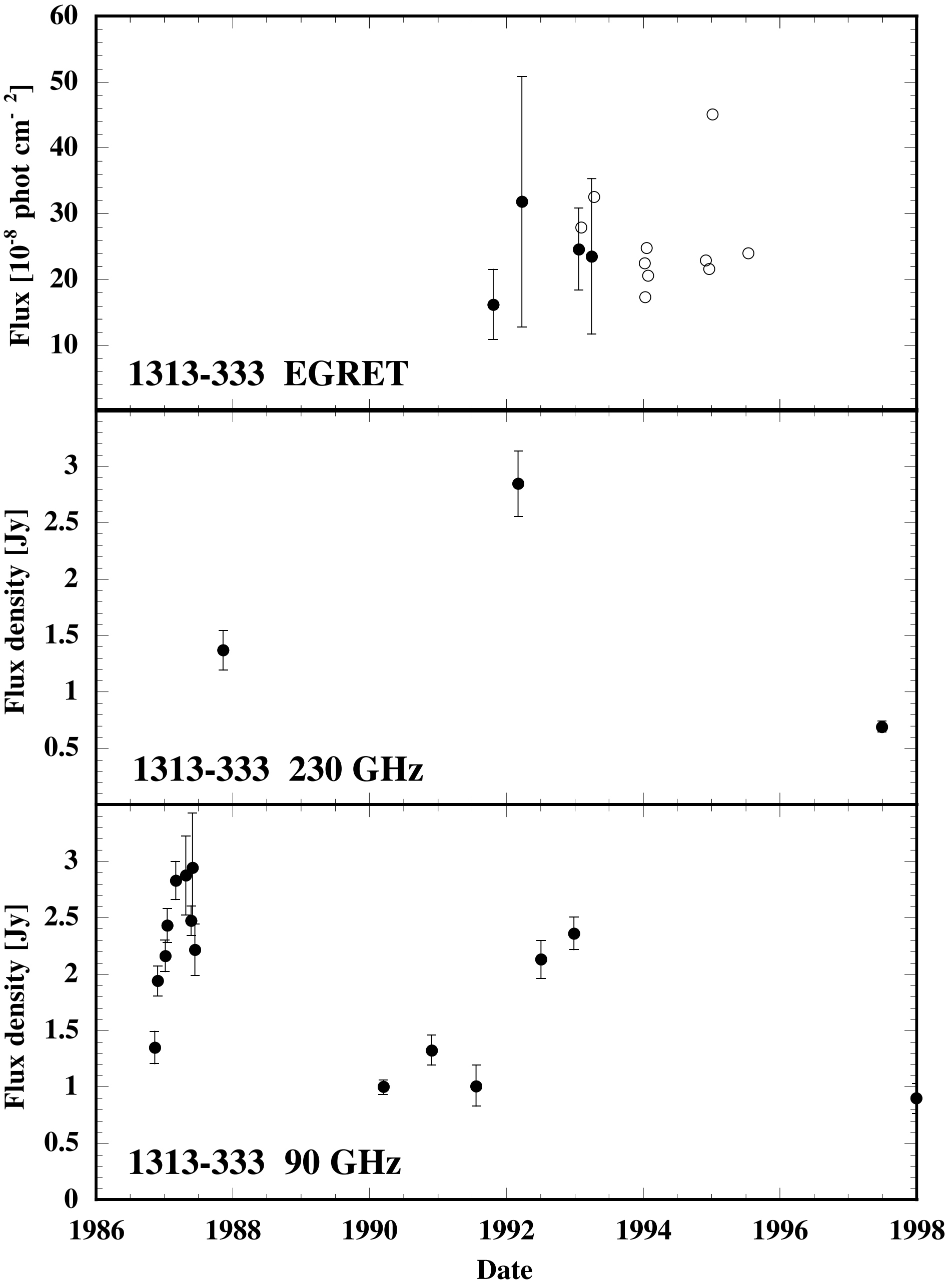

Fig. 11.— As Fig. 5 but for the source B1313−333.

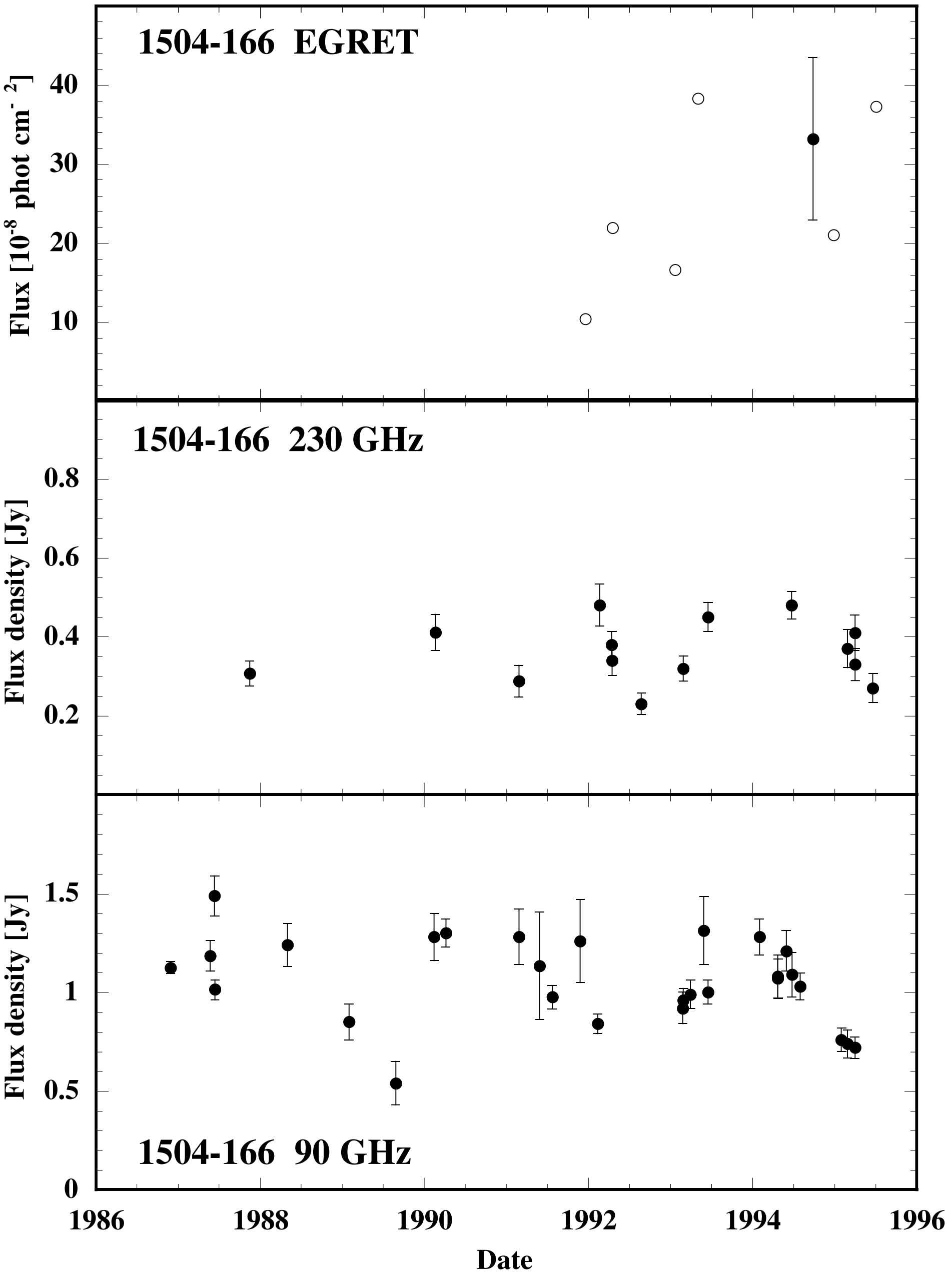

Fig. 12.— As Fig. 5 but for the source B1504−166.

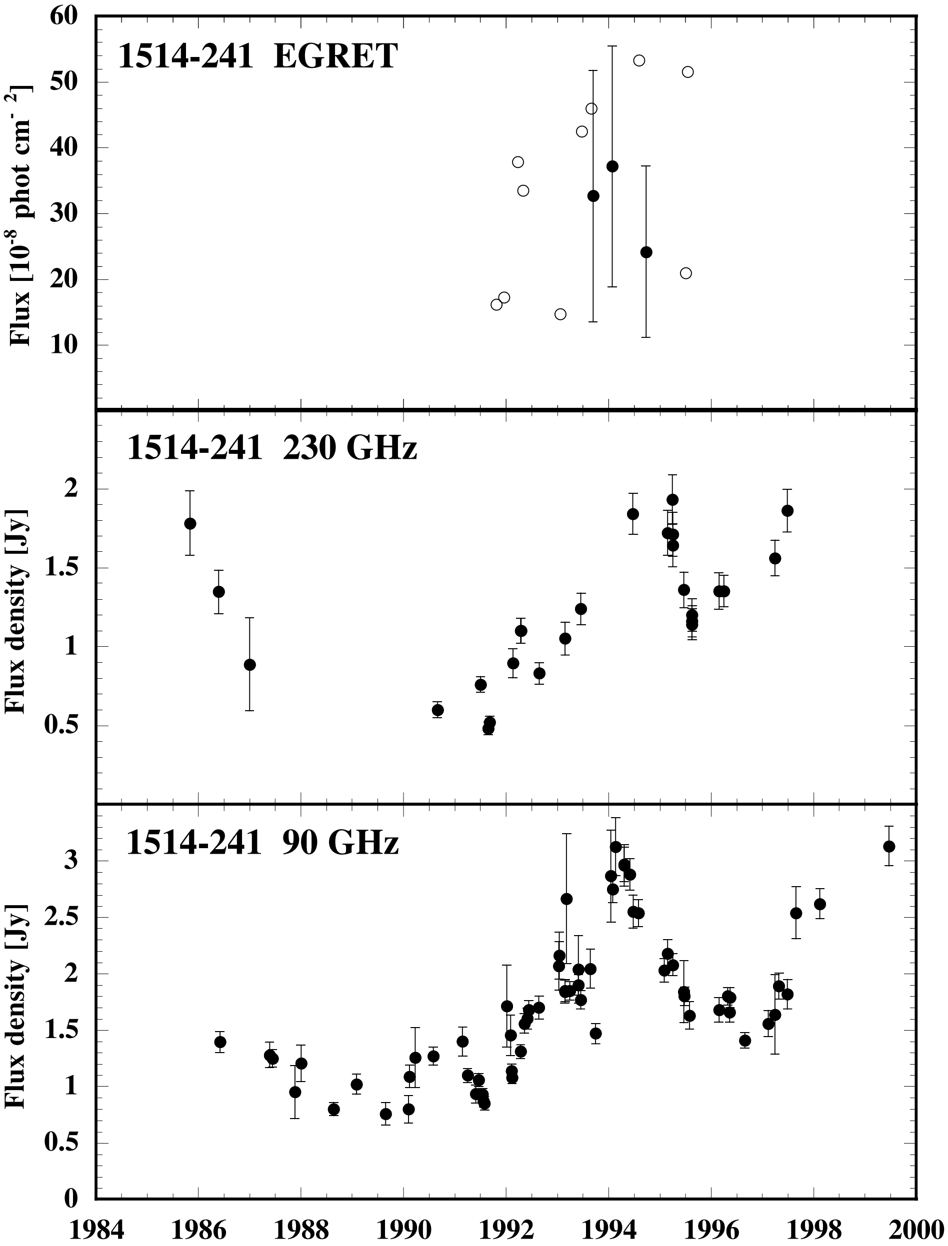

Fig. 13.— As Fig. 5 but for the source B1514−241.

Table 1. 3EG High-confidence identifications with AGNs (= the sources marked as "A" (an AGN) in 3EG).

AGN	S_{5min} (Jy)	S_{5max} (Jy)	N_5	S_{22min} (Jy)	S_{22max} (Jy)	N_{22}	S_{90min} (Jy)	S_{90max} (Jy)	N_{90}	$\alpha_{5-90,q}$	$\alpha_{5-90,a}$	$\alpha_{5-22,a}$	$\alpha_{22-90,a}$
B0202+149	2.30	3.55	28	1.45	4.79	84	0.79	3.71	56	-0.37	+0.01	+0.20	-0.18
B0208-512	2.84	3.54	8				1.19	6.51	59	-0.30	+0.21		
B0219+428	1.19	1.22	3	0.42	1.40	25	0.73	1.04	3	-0.17	-0.06	+0.09	-0.21
B0235+164	0.93	4.18	55	0.73	6.10	164	0.45	6.32	161	-0.25	+0.14	+0.26	+0.03
B0336-019	2.24	3.45	13	1.13	3.93	29	1.08	3.16	69	-0.25	-0.03	+0.09	-0.16
B0414-189	1.09	1.35	7	0.53	0.53	1	0.42	0.88	4	-0.33	-0.15	-0.63	+0.36
B0420-014	1.46	8.37	44	2.15	7.55	149	1.39	9.04	199	-0.02	+0.03	-0.07	+0.13
B0430+2859	0.48	0.48	2				0.22	0.40	3	-0.27	-0.06		
B0440-003	1.35	3.39	12	0.91	1.55	10	0.43	1.23	26	-0.40	-0.35	-0.53	-0.16
B0446+112	0.58	1.77	13	0.59	2.18	21	0.46	1.67	17	-0.08	-0.02	+0.14	-0.19
B0454-234	1.36	2.68	22	1.80	3.90	10	0.56	2.27	47	-0.31	-0.06	+0.25	-0.38
B0454-463	1.84	2.97	4				0.60	2.60	15	-0.39	-0.05		
B0458-020	1.70	3.53	30	1.01	4.28	61	0.41	3.86	55	-0.49	+0.03	+0.13	-0.07
B0459+060	0.78	0.78	1	0.52	0.52	1						-0.27	
B0528+134	1.45	5.66	43	1.51	11.30	123	0.90	8.23	101	-0.17	+0.13	+0.47	-0.23
B0537-441	3.80	5.22	13				1.50	7.99	51	-0.32	+0.15		
B0616-116	0.26	0.29	2										
B0716+714	0.47	0.78	22	0.24	2.21	51	0.46	2.75	84	-0.01	+0.44	+0.70	+0.16
B0735+178	1.45	2.99	19	0.66	5.16	148	0.40	3.92	101	-0.45	+0.09	+0.37	-0.19
B0738+5451	0.27	0.27	1	0.12	0.37	3						+0.21	
B0827+243	0.60	1.13	18	0.89	1.58	14	0.55	3.27	15	-0.03	+0.37	+0.23	+0.52
B0829+046	0.70	1.13	3	1.09	1.09	1	1.20	1.20	1	0.19	+0.02	-0.02	+0.07
B0836+710	1.87	2.59	26	0.57	2.74	36	0.53	1.30	7	-0.44	-0.24	+0.04	-0.53
J0850-1213							0.48	1.22	6				
B0851+202	1.74	3.34	12	1.26	6.70	207	0.90	8.65	216	-0.23	+0.33	+0.47	+0.18
B0954+556	2.06	2.28	2	0.32	1.44	28	0.51	0.55	3	-0.48	-0.49	-0.31	-0.68
B0954+658	0.58	1.46	10	0.40	1.68	46	0.74	1.81	11	+0.08	+0.07	+0.09	+0.05
B1101+384	0.57	0.78	21	0.20	1.03	106	0.27	0.91	17	-0.26	+0.05	+0.19	-0.09
B1156+295	1.34	1.61	5	0.75	3.52	129	0.47	5.09	73	-0.36	+0.40	+0.53	+0.26
B1219+285	0.58	0.96	8	0.20	3.06	28	0.24	0.92	20	-0.31	-0.02	+0.78	-0.85
B1222+216	0.81	1.13	2	1.51	2.59	31	0.67	1.69	27	-0.07	+0.14	+0.56	-0.30
B1226+023	33.40	44.59	41	20.13	59.00	441	8.63	42.06	353	-0.47	-0.02	+0.19	-0.24
B1229-021	0.90	1.10	14	0.79	1.16	3	0.20	0.41	7	-0.52	-0.34	+0.04	-0.74
B1243-072	0.61	1.40	7	0.74	1.30	2	0.56	0.67	3	-0.03	-0.25	-0.05	-0.47
B1253-055	9.40	16.58	46	7.97	34.02	323	5.48	30.85	218	-0.19	+0.21	+0.49	-0.07

Table 1—Continued

AGN	S_{5min} (Jy)	S_{5max} (Jy)	N_5	S_{22min} (Jy)	S_{22max} (Jy)	N_{22}	S_{90min} (Jy)	S_{90max} (Jy)	N_{90}	$\alpha_{5-90,q}$	$\alpha_{5-90,a}$	$\alpha_{5-22,a}$	$\alpha_{22-90,a}$
B1331+170	0.71	0.71	1	0.23	0.23	1						-0.76	
B1334-127	2.18	5.07	4	4.10	7.70	2	2.04	9.35	116	-0.02	+0.21	+0.28	+0.14
B1406-076	0.58	1.08	16	0.60	1.97	19	0.39	1.39	29	-0.14	+0.09	+0.41	-0.25
B1424-418	2.12	4.08	10				1.63	5.59	5	-0.09	+0.11		
B1510-089	1.75	4.03	34	1.05	6.30	107	0.74	6.22	112	-0.30	+0.15	+0.30	-0.01
B1604+159	0.51	0.51	1										
B1606+106	1.08	1.84	22	0.50	1.70	17	0.39	1.68	23	-0.35	-0.03	-0.05	-0.01
B1611+343	2.20	3.75	22	1.44	5.37	90	0.70	3.23	18	-0.40	-0.05	+0.24	-0.36
B1622-253	1.84	2.35	4	5.29	5.29	1	1.05	4.45	8	-0.19	+0.22	+0.55	-0.12
B1622-297	1.70	2.25	5	3.15	3.15	1	1.34	7.67	27	-0.08	+0.42	+0.23	+0.63
B1633+382	1.79	4.02	33	1.11	3.71	194	0.72	2.84	59	-0.32	-0.12	-0.05	-0.19
B1725+044	1.21	1.25	2	0.27	1.30	38						0.03	
B1730-130	4.10	5.43	7	6.45	11.23	8	2.27	12.47	93	-0.20	+0.29	+0.49	+0.07
B1739+522	0.73	2.57	13	0.56	3.88	65	0.80	2.23	10	+0.03	-0.05	+0.28	-0.39
B1741-038	2.12	4.03	28	1.02	5.66	77	1.24	6.28	95	-0.19	+0.15	+0.23	+0.07
B1759-396													
B1830-210	8.88	10.24	2				1.42	6.10	45	-0.63	-0.18		
B1908-201	2.46	2.46	1	2.70	2.70	1	1.10	3.34	12	-0.28	+0.11	+0.06	+0.15
B1933-400	0.70	1.48	3				0.49	1.13	9	-0.12	-0.09		
B1936-155	0.96	1.69	7	0.80	2.03	2	0.55	1.49	15	-0.19	-0.04	+0.12	-0.22
B2022-077	0.89	0.89	1										
B2032+107	0.77	0.77	1	0.94	0.94	1						+0.13	
B2052-474	2.45	2.52	2				0.93	1.86	9	-0.34	-0.11		
B2155-304	0.30	0.53	4				0.17	0.53	19	-0.20	+0.00		
B2200+420	2.40	4.81	9	1.23	12.70	378	1.13	6.53	135	-0.26	+0.11	+0.66	-0.47
B2209+236	0.80	0.80	1	0.90	0.90	1						+0.08	
B2230+114	3.50	4.22	30	1.39	5.50	114	1.17	8.33	94	-0.38	+0.24	+0.18	+0.29
B2251+158	8.70	24.00	37	5.09	17.60	314	4.02	15.51	209	-0.27	-0.15	-0.21	-0.09
B2320-035	0.80	0.80	1	0.56	0.56	1	0.55	0.59	2	-0.13	-0.11	-0.24	+0.04
B2351+456	1.42	1.42	1										
B2356+196	0.54	0.75	16	0.35	0.35	1		< 0.20	4			-0.52	

Table 2. 3EG Lower-confidence identifications with Southern AGNs (= the sources marked as "a" (possible AGN) in 3EG).

AGN	S_{5min} (Jy)	S_{5max} (Jy)	N_5	S_{22min} (Jy)	S_{22max} (Jy)	N_{22}	S_{90min} (Jy)	S_{90max} (Jy)	N_{90}	$\alpha_{5-90,q}$	$\alpha_{5-90,a}$	$\alpha_{5-22,a}$	$\alpha_{22-90,a}$
B0130−171	0.62	1.00	4	0.80	0.80	1	0.40	1.76	2	−0.15	+0.20	−0.15	+0.56
B0506−612	1.46	2.11	4				0.96	1.43	8	−0.15	−0.13		
B0521−365	8.75	9.88	13				1.90	5.43	34	−0.53	−0.21		
B0537−286	0.99	1.02	2	1.10	1.10	1	0.39	0.58	3	−0.32	−0.20	+0.05	−0.45
B0539−057	1.31	1.56	5	1.40	1.40	1	0.38	0.50	3	−0.43	−0.39	−0.07	−0.73
B0805−077	1.01	1.04	2	2.47	2.47	1	0.82	2.45	18	−0.07	+0.30	+0.58	−0.01
B1127−145	3.29	5.62	11	1.54	6.30	7	0.66	2.15	13	−0.56	−0.33	+0.08	−0.76
B1313−333	1.32	1.36	2				0.90	2.94	15	−0.13	+0.27		
B1504−166	1.93	3.17	13	2.20	2.40	2	0.54	1.49	27	−0.44	−0.26	−0.13	−0.40
B1514−241	1.20	2.29	16	1.70	3.30	3	0.76	3.13	65	−0.16	+0.11	+0.25	−0.04
B1716−771								<0.37	1				
J1808−5011								<0.25	1				
B1920−211	2.88	2.88	1	2.46	2.46	1						−0.11	

Table 3. Promising candidates for new southern EGRET identifications from Mattox et al. (1997) (MSM).

AGN	Candidate for	90 GHz epoch	$S_{90,max}$ (Jy)	$\alpha_{5,90}$
J1249-8303	2EG 1248-8308	2000.329	N.D.	
J1650-5044	2EG 1648-5042	2000.329	1.655 ± 0.105	-0.02

Table 4. Possible candidates for new southern EGRET identifications from Mattox et al. (1997) (MSM).

AGN	Candidate for	90 GHz epoch	$S_{90,max}$ (Jy)	$\alpha_{5,90}$
J0156-3616	2EG 0159-3557	2000.630	N.D.	
J0159-3604	2EG 0159-3557	2000.630	N.D.	
J0719-5228	2EGS 0724-5157	2000.329, 2000.630	N.D.	
J0724-5235	2EGS 0724-5157	2000.329	N.D.	
J0718-4711	2EG 0720-4746	2000.329	N.D.	
J0726-4728	2EG 0720-4746	2000.630	0.340 ± 0.077	-0.19
J1057-7724	2EGS 1050-7650	2000.630	N.D.	
J1058-8003	2EGS 1050-7650	1997.99, 2000.63	1.638 ± 0.177	-0.09
J1454-1925	2EG 1457-1916	2000.630	0.191 ± 0.080, S/N=2.4	-0.21
J1634-1440	2EG 1635-1427	2000.630	N.D.	
J1641-2728	2EGS 1641-2659	2000.630	N.D.	
J1647-6437	2EGS 1703-6302	2000.630	0.370 ± 0.082	-0.44
J1703-6212	2EGS 1703-6302	2000.329	1.227 ± 0.136	$+0.24$
J1710-0355	2EG 1709-0350	2000.630	N.D.	
J1713-0817	2EGS 1708-0927	2000.630	N.D.	
J1743-2247	2EG 1742-2250	2000.630	N.D.	
J1750-0841	2EG 1746-0935	2000.329	N.D.	
J1849-2638	2EG 1850-2638	2000.329	N.D.	
J2005-2310	2EG 2006-2253	2000.630	0.253 ± 0.125, S/N=2.1	-0.01

Table 5. Possible candidates for new southern EGRET identifications of the previously unidentified 3EG sources

AGN	Candidate for	90 GHz epoch	$S_{90,max}$ (Jy)	$\alpha_{5,90}$
J0617-3259	3EG J0616-3310	2000.329	N.D.	
J0657-6139	3EG J0702-6212	2000.329, 2000.630	N.D.	
J0710-3850	3EG J0706-3837	2000.329, 2000.630	0.252 ± 0.090, S/N=2.8	-0.19
J0821-5800	3EG J0821-5814	2000.329, 2000.630	N.D.	
J0825-5849	3EG J0821-5814	2000.329, 2000.630	N.D.	
J1302-4350	3EG J1300-4406	2000.329	N.D.	
J1302-4446	3EG J1300-4406	2000.329	N.D.	
J1302-4447	3EG J1300-4406	2000.329, 2000.630	0.243 ± 0.072, S/N=3.4	-0.25
J1254-4425	3EG J1300-4406	2000.329, 2000.630	0.379 ± 0.100, S/N=3.8	$+0.03$
J1502-3520	3EG J1500-3509	2000.329	N.D.	
J1457-3539	3EG J1500-3509	2000.329	N.D.	
J1457-3538	3EG J1500-3509	2000.329	N.D.	
J1505-3432	3EG J1500-3509	2000.329	N.D.	
J1605-1139	3EG J1607-1101	2000.63	0.530 ± 0.085	$+0.12$
J1632-1052	3EG J1631-1018	2000.63	N.D.	
J1647-0715	3EG J1646-0704	2000.63	N.D.	
J1802-0207	3EG J1800-0146	2000.63	N.D.	
J1819-6345	3EG J1813-6419	2000.63	0.537 ± 0.084	-0.73
J2249-1251	3EG J2251-1341	2000.63	0.208 ± 0.095, S/N=2.2	-0.15